Construction of human BMP2-IRES-HIF1α^{mu} adenovirus expression vector and its expression in mesenchymal stem cells

DANPING LIU[1], LIANG HU[2], ZHENG ZHANG[1], QUAN YING LI[1] and GUOXIAN WANG[3]

[1]Department of Bone and Joint Surgery, First Affiliated Hospital of Liaoning Medical University, Jinzhou, Liaoning 121000;
[2]Department of Orthopaedics, the First People's Hospital of Jingmen, Hubei 448000;
[3]Department of Pharmacology, Liaoning Medical University, Jinzhou, Liaoning 121000, P.R. China

Received July 5, 2012; Accepted November 6, 2012

DOI: 10.3892/mmr.2012.1237

Abstract. The present study aimed to construct a novel recombinant adenovirus expression vector Ad-BMP2-IRES-HIF1α^{mu} that expresses human bone morphogenetic protein (BMP2) and mutant hypoxia-inducible factor 1α, and investigated its effects in promoting neogenesis of bone and angiogenesis. The recombinant adenovirus BMP2, HIF1α^{mu} and pIRES2-EGFP expression vectors were constructed and transfected into HEK293A cells. The groups were divided into group A, transfection with Ad-BMP2-IRES-HIF1α^{mu}; group B, transfection with Ad-HIF1α^{mu}-IRES-hrGFP-1; group C, transfection with Ad-BMP2-IRES-hrGFP-1; group D, transfection with Ad-IRES-hrGFP-1; group E, not transfected. Adenovirus liquid was transferred into rabbit mesenchymal stem cells (MSCs) pretreated with dexamethasone at the best multiplicity of infection (MOI). The mRNA and protein expression of BMP2 and HIF1α were detected by RT-PCR and western blot analysis. Adenovirus was successfully packaged. The expression level of HIF1α mRNA in group A and B was markedly higher than that in groups C, D and E, showing a significant difference ($P<0.01$). There was a significant difference in the expression level of BMP2 mRNA between group A and C ($P<0.05$) and this was markedly higher than that in groups B, D and E ($P<0.01$). The protein expression level of HIF1α in group A and B was markedly higher than that in groups C, D and E ($P<0.01$). The protein expression level of BMP2 in group A and C was markedly higher than that in groups B, D and E ($P<0.01$). The human BMP2-IRES-HIF1α^{mu} adenovirus expression vector was successfully constructed and the experimental groups formed bone and blood vessels prior to the positive and negative control groups.

Correspondence to: Professor Guoxian Wang, Department of Pharmacology, Liaoning Medical University, Jinzhou 121000, P.R. China
E-mail: klcn198@163.com

Key words: bone morphogenetic protein 2, hypoxia-inducible factor 1, bone marrow mesenchymal stem cells

Introduction

Bone defects and non-union caused by various diseases, such as trauma and tumors, are common orthopedic disorders in the clinic. Treatment is limited by the finite nature of autogenous bone materials; however, with the rise of tissue engineering, this problem may be solved using new methods. Current research (1-3) shows that bone morphogenetic protein (BMP) belongs to the TGF-β superfamily, which plays a notable role in inducing bone differentiation. Among its family members, BMP2 is one of the strongest factors and the only growth factor that is capable of singly inducing bone formation. HIF1 expression was increased in low oxygen environments, and it could be combined with the hypoxia response element of target genes, regulate gene transcription of vascular endothelial growth factor (VEGF), and play a crucial role in tissue angiogenesis (4-7). The current study will build a recombinant adenovirus vector containing a BMP2 and three mutant HIF1α (HIF1α^{mu}) (Ad-BMP2-IRES-HIF1α^{mu}), to be transfected into rabbit bone marrow mesenchymal stem cells (MSCs), and observe the mRNA and protein expression of the two genes in the MSCs which will provide support for gene therapy of clinical bone defects and bone non-union.

Materials and methods

Primers. Primer sequences were designed according to the sequence information of the target gene human BMP2 and the HIF1α^{mu} gene and the enzyme digestion site information of the pIRES2-EGFP vector. *Nhe*I and *Bam*HI sites were respectively added at the 5' end and the 3' end of BMP2 primer, and a 6xHIS tag was added at the C-cleavage site of the BMP2 gene.*Bst*XI and *Xba*I sites were respectively added at the 5' end and 3' end of the HIF1α^{mu} primer, and a 3xFlag tag was added at the C-cleavage site. The study was approved by the ethics committee of Liaoning Medical University, Liaoning, China.

Vector construction. The HIF1α^{mu} fragment was amplified by PCR using pShuttle-CMV-HIF1α^{mu}-IRES-hrGFP-1 plasmid as the template. The target fragment was recovered and double enzyme digested with *Bst*XI and *Xba*I. The vector pIRES2-EGFP was double enzyme digested with *Bst*XI and *Xba*I and recovered by agarose gel electrophoresis. The BMP2

fragment was amplified by PCR with pShuttle-CMV-BMP2 plasmid as the template. The target fragment was double enzyme digested with *Nhe*I and *Bam*HI and recovered by agarose gel electrophoresis. The correct pIRES2-HIF11α^{mu}-flag vector was double enzyme digested with *Nhe*I and *Bam*HI and the larger fragment was recovered. The previously mentioned enzyme was digested and the recovered target gene was ligated with the vector fragment for 2 h at 22˚C, and then transformed into competent *E. coli* DH5α.

Screening and identifying of positive clones. The positive clones identified by colony PCR were transferred into Kan-LB and agitated overnight at 37˚C, and then the plasmid was extracted the next day. The positive clones screened by colony PCR and enzyme digestion were sequenced. The confirmed clones were stored.

Recombination of adenovirus expression vector. BMP2-IRES-HIF1α^{mu} recombinant fragment was amplified with BMP2-pIRES2-HIF1α^{mu} vector as the template and then recovered. The target fragment BMP2-IRES-HIF1α^{mu} was recombined to the pDONR221 vector using the BP recombinant system of Invitrogen (Carlsbad, CA, USA). The target sequence BMP2-IRES-HIF1α^{mu} was recombined to adenovirus vector pAd-BMP2-IRES-HIF1α^{mu} using the LP recombinant system of Invitrogen. The recombinant plasmids were sequenced, and stored at -20˚C until further use.

Titration of virus liquid. The target gene was transferred into HEK293 cells in the exponential phase and the transfer process was observed under a fluorescence microscope. An end-point dilution assay was used to determine the titer of virus liquid.

Recombinant adenovirus transfection of rabbit MSCs. Group A (experimental group): transfection with Ad-BMP2-IRES-HIF1α^{mu}; group B (positive control group 1): transfection with Ad-HIF1α^{mu}-IRES-hrGFP-1; group C (positive control group 2): transfection with Ad-BMP2-IRES-hrGFP-1; group D (negative control group): transfection with Ad-IRES-hrGFP-1; group E (blank group): without transfection virus.

Rabbit MSCs within three generations were digested by trypsin and mixed, then transferred into 6-well plates at a density of 5x10^5/well, with routine culture for 24 h in a cell culture box. The supernatant was discarded following firm adherence.

Multiplicity of infection (MOI) = (pfu/ml value) x (virus liquid volume)/(cell number for transfection). Virus liquids at MOI of 50, 100, 150 and 200 were respectively transferred into MSCs, leaving two wells as the negative controls. Following incubation for 1 h at 37˚C, the cells were routinely cultured for 48-72 h with complete medium and then observed under the inversion fluorescence microscope.

Every virus liquid in each group was respectively transferred into rabbit MSCs at its best MOI value. The largest MOI not causing a marked cytopathic effect was considered as the best MOI. In this experiment, the best MOI=100. Fresh serum medium (2 ml) was respectively added to each flask of cells, and cells were cultured for 3 h in a constant temperature cell culture box, then an additional 2 ml medium was added to each flask of cells, with continued culture for 24-72 h. The transfer effect was observed under the inversion fluorescence microscope.

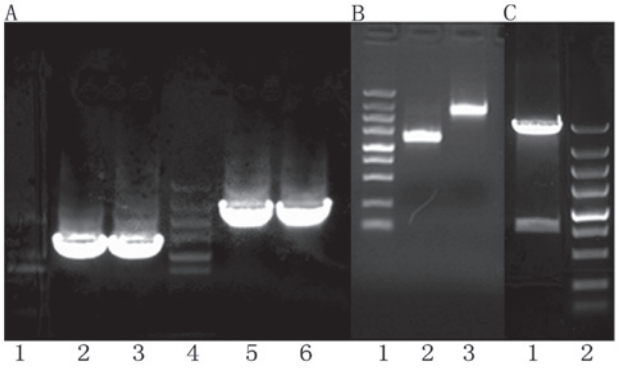

Figure 1. (A) PCR amplification of muHIF1 and BMP2 genes. Lane 1: DL2000 marker; Lanes 2-3: BMP2 gene (1.2 k); Lane 4: DL5000 marker; Lanes 5-6: muHIF1 gene (target strip 2.5 KB). (B) Enzyme digestion of muHIF1 and BMP2. Lane 1: DL5000 marker; Lane 2: BMP2 (1.2 k); Lane 3: muHIF1 (4.8 k). (C) Enzyme digestion of pIRES2-EGFP vector. Lane 1: pIRES2-EGFP (4.8 k + 426 bp); Lane 2: DL5000 marker.

RT-PCR. Total RNA was extracted according to a kit that contained 2 μl PrimeScript 1 Step Enzyme Mix and 25 μl 2X 1 Step Buffer (Dye Plus). Then 2 μl upstream primer and 2 μl downstream primer, 1 μl total RNA and 18 μl RNase-free ddH_2O were added to make up the 50 μl RT-PCR reaction solution. The RT-PCR reaction was as follows: a cycle of 50˚C for 30 min; a cycle of 94˚C for 2 min; 30 cycles of 94˚C for 30 sec, 60˚C for 30 sec and 72˚C for 1 min. After the reaction, 5-8 μl reaction solutions underwent 1% agarose gel electrophoresis for 40 min. The electrophoresis results were observed and the OD value of strips was detected using a gel imaging system. This was repeated for three times, and the relative OD values were separately calculated.

Western blot analysis. Cellular total protein in each group was extracted using cellular protein lysis buffer, and the protein concentration in each group was detected by BCA; 5% spacer gel and 8% separation gel were prepared for polyacrylamide gel electrophoresis at 60 V for 30 min, and then 150 V for 1 h. Following electrophoresis, the separation gel was washed three times and then placed in a transfer box at 100 mA for 30 min. The film was then incubated with the primary antibodies (1:1500) overnight at 4˚C. The film was then washed and then incubated with the secondary antibodies and developer solution for 30 min at room temperature, avoiding light. The film was then washed with eluent three times to terminate the chromogenic reaction. The OD value of target strips and internal reference on the film were analyzed using a gel imaging system. The experiment was repeated three times, and the relative OD values were calculated.

Statistical analysis. The experimental data were statistically analyzed using SPSS17.0 software. Measurement data were expressed as the means ± standard deviation (±s) and analyzed by one-way analysis of variance. $P<0.05$ was considered to indicate a statistically significant difference.

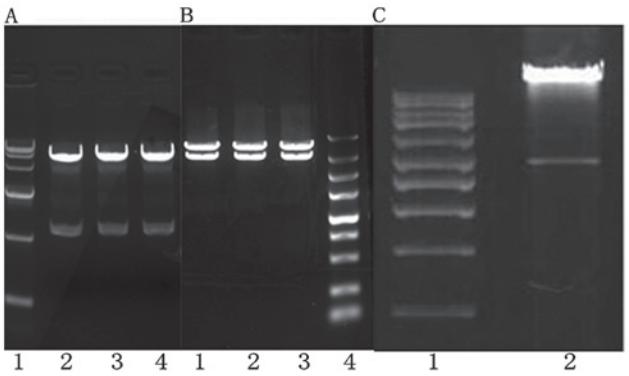

Figure 2. (A) Identification of recombinant PBMP2-IRES-muHIF by enzyme digestion. Lane 1: DL15000 marker; Lane 2-4: pBMP2-IRES-muHIF recombination (7 k + 1.2 k). (B) Identification of recombinant PIRES2-muHIF1-Flag by enzyme digestion. Lane 1-3: pIRES2-muHIF1-Flag recombinant (4 k + 3 k); Lane 4: DL5000 marker. (C) Identification results of eukaryotic expression vector of recombinant adenovirus by enzyme digestion with *Pac*I. Lane 1: DL10000 marker; Lane 2: Target gene.

Results

Recombinant identification. A 9789 bp recombinant plasmid strip, a 1191 bp BMP2 strip and a 2481 bp HIF1α strip were observed after agarose gel electrophoresis, and the zymogram analysis of recombinant plasmid was the same as expected. The BMP2 fragment and the HIF1α fragment in the recombinant plasmid completely coincided with the BMP2 (NM001200) CDS area and the HIF1α (NM001530) CDS area in Genebank, respectively, with insert fragments in the correct direction (Figs. 1 and 2A and B).

Adv-BMP-2-IRES-HIF1α^{mu} identification. There were two strips at 3000 and 10000 bp as shown by agarose gel electrophoresis following enzyme digestion, which indicated that the shuttle plasmid had been successfully ligated to the adenovirus genome and Adv-BMP-2-IRES-HIF1α^{mu} had been successfully constructed. The target fragment BMP2 was detected by RT-PCR and agarose gel electrophoresis, and there was a strip at 1191 bp, which is the same as expected. The target fragment HIF1α was detected by RT-PCR and agarose gel electrophoresis, and there was a strip at 2481 bp, which was the same as expected (Fig. 2C).

Transfer and titration of virus liquid. Under inverted fluorescence microscopy, the majority of cells appeared green and cell fragments had become detached and showed a cytopathic effect. The titer of virus liquid was $3.16x10^8$ according to the end-point dilution assay (Fig. 3A and B).

Cell culture. After the original cultivation of rabbit bone marrow stromal cells for one week, there was cell adherence to the wall when the culture solution was changed. Cells were passaged when they reached 80% confluence. The third generation had a higher purity and a good adhesion (Fig. 3C and D).

RT-PCR. There was no marked difference in the HIF1α mRNA expression level between group A and B (P>0.05), with the same result among groups C, D and E (P>0.05). The HIF1α mRNA expression level in group A and B was markedly higher than that in groups C, D and E, with a significant difference (P<0.01). There was a significant difference in BMP2 mRNA expression level between group A and C (P>0.05), but no marked difference among groups B, D and E (P>0.05). The BMP2 mRNA expression level in group A and C were markedly higher than that in groups B, D and E, with a significant difference (P<0.01) (Fig. 4A and B, Table I).

Western blot analysis. The HIF1α protein expression level in group A and B was significantly higher than that in the other three groups, with a significant difference (P<0.01). However, there was no significant difference among groups C, D and E

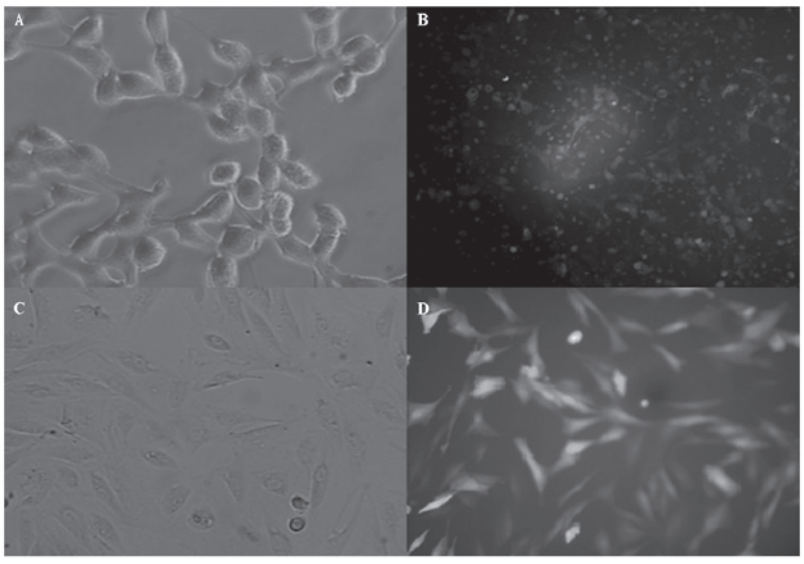

Figure 3. (A) Normally recovered HEK293 cells with 50% confluence (x40). (B) Observation of HEK293 cells following transfer of recombinant adenovirus for 3 days under a fluorescence microscope (x40). (C) The third generation of rabbit bone marrow stromal cells with 80% confluence (x40). (D) Observation of rabbit bone marrow stromal cells following transfer of recombinant adenovirus for 3 days under fluorescence microscope (x40).

Table I. OD value of β-actin, BMP2 and HIF1α detected by RT-PCR (mean ± SD).

Group	Group A	Group B	Group C	Group D	Group E
β-actin	7.73±0.09	7.75±0.09	7.52±0.30	7.39±0.29	7.48±0.06
HIF1α	7.10±0.10	7.18±0.23	2.08±0.18	2.25±0.23	2.34±0.29
BMP2	8.13±0.08	2.18±0.15	6.20±0.05	2.18±0.18	2.14±0.09
HIF1α relative OD value	0.92±0.02	0.93±0.04	0.28±0.03	0.30±0.02	0.31±0.04
BMP2 relative OD value	1.05±0.01	0.28±0.02	0.82±0.03	0.29±0.04	0.29±0.03

Table II. OD value of β-actin, BMP2 and HIF1α detected by western blot analysis (mean ± SD).

Group	Group A	Group B	Group C	Group D	Group E
β-actin	2.93±0.09	2.98±0.11	2.99±0.21	2.95±0.12	2.90±0.07
HIF1α	1.02±0.14	1.12±0.18	0.18±0.08	0.18±0.12	0.17±0.13
BMP2	1.51±0.02	0.18±0.14	1.02±0.23	0.18±0.14	0.17±0.14
HIF1α relative OD value	0.35±0.03	0.38±0.02	0.06±0.03	0.06±0.04	0.06±0.04
BMP2 relative OD value	0.52±0.02	0.06±0.05	0.34±0.03	0.06±0.02	0.06±0.04

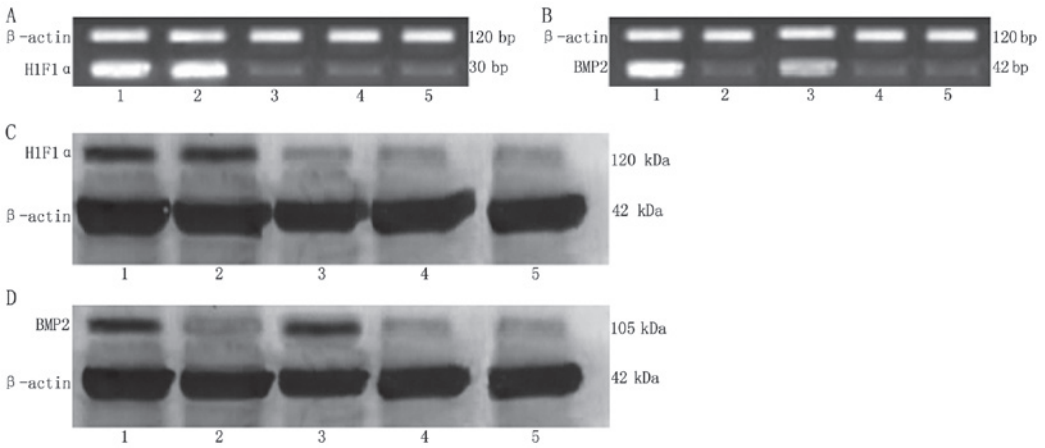

Figure 4. (A) Expression of HIF1α and β-actin in each group of cells was detected by RT-PCR. (B) Expression of BMP2 and β-actin in each group of cells was detected by RT-PCR. (C) Protein expression of HIF1α and β-actin in each group of cells was detected by western blot analysis. (D) Protein expression of BMP2 and β-actin in each group of cells was detected by western blot analysis.

(P>0.1). BMP2 protein expression level in group A and C was significantly higher than that in the other three groups, with a significant difference (P<0.01). However, there was no significant difference among groups B, D and E (P>0.1). There was also a significant difference in the BMP2 protein expression level between group A and C (P<0.05) (Fig. 4C and D, Table II).

Discussion

Previous studies reported that the incidence rate of delayed union after fracture and non-union was approximately 5-10%, and treatment of this remains a big problem in the field of orthopedics (8-10). In the BMP family, BMP2 is the main signaling protein regulating bone formation (11-13). BMP2 could induce differentiation of pluripotent mesenchymal progenitor cells into osteoblast cells, promoting bone formation of osteoblast cells. There were also studies confirming that BMP2 was capable of inducing pluripotent mesenchymal progenitor cells to differentiate into osteoblast cells *in vitro* or *in vivo* (14-15). During the process of bone defect and fracture healing, BMP2 promoted the osteogenetic effect at the fracture site, but following osteoblast induction, the lack of blood supply at the fracture site and difficult angiogenesis affected the repair process of the fracture.

It has been demonstrated that the activating transcription factor HIF1α found in recent years is capable of activating low oxygen metabolism and regulating the transcription of angiogenesis-promoting genes. At the same time it also participates in the regulation of VEGF and SDF21 expression (16). Therefore, HIF1α has been considered as one of the most promising genes in the clinical application of promoting angiogenesis. However, HIF1α loses its transcription activity due to its easy degradation under usual oxygen conditions

(17-19). Liu *et al* (20) successfully constructed recombinant adenovirus-mediated mutations of hypoxia inducible factor expression vector (HIF1α^{mu}), which could be expressed under usual oxygen conditions and rapidly accumulate in cells and promote angiogenesis. The double gene co-expression of the adenovirus vector with BMP2 and HIF1α^{mu} constructed in this experiment was expected to form a cooperative effect due to the expression of both genes (7), accelerating the repair process of fractures and bone defects. The past use of a single gene vector had a poor treatment effect, and conjunction with many genes and vectors often increased dosages of adenovirus and virus infection efficiency (20). The advantage of two genes with a single vector constructed in this experiment was the reduction of the dosage of adenovirus required during bone defect treatment.

According to the results of RT-PCR and western blot analysis, the expression level of HIF1α mRNA was significantly increased following transfection into MSCs in group B. The expression level of BMP2 mRNA was significantly increased following transfection into MSCs in group C. The expression level of BMP2 mRNA and HIF1α mRNA were both not increased following transfection into MSCs in group D and E, demonstrating that it was not adenovirus expression vector itself or hrGFP-1 that caused the increased expression level of BMP2 and HIF1α mRNA. The expression levels of HIF1α mRNA and BMP2 mRNA were significantly increased at the same time after transfection into MSCs in group A, and the expression of BMP2 was higher than that in group C. There was no significant difference in HIF1α expression between group A and B, indicating that mutant HIF1α was likely to promote the osteogenetic function of BMP2, which would provide a new direction for angiogenic treatment of bone defect diseases. This point was consistent with the experimental results we had expected.

The angiogenesis process in the osteogenesis system is an extremely complex physical process. Importing mutations of the HIF1α gene was an abnormal way to normalize tissue, and promoted the formation of a new vascular network, but with an unknown effect on other factors themselves participating in the process of angiogenesis. The effect of mutant genes on HIF1α itself will also require further research.

Acknowledgements

This study was supported by the Key talent project of Liaoning Provincial Health Bureau, China (No. 2010921045).

References

1. Jorgensen NR, Henriksen Z, Sorensen OH and Civitelli R: Dexamethasone, BMP-2, and 1, 25-dihydroxyvitamin D enhance a more differentiated osteoblast phenotype: validation of an in vitro model for human bone marrow-derived primary osteoblasts. Steroids 69: 219-226, 2004.
2. Shin JH, Kim KH, Kim SH, *et al*: Ex vivo bone morphogenetic protein-2 gene delivery using gingival fibroblasts promotes bone regeneration in rats. J Clin Periodontol 37: 305-311, 2010.
3. Cheng H, Jiang W, Phillips FM, *et al*: Osteogenic activity of the fourteen types of human bone morphogenetic proteins (BMPs). Bone Joint Surg Am 85: 1544-1552, 2003.
4. Wan C, Gilbert SR, Wang Y, *et al*: Activation of the hypoxia-inducible factor-1-alpha pathway accelerates. Proc Nat Acad Sci U S A 105: 686-691, 2008.
5. Hua Z, Nicola JM, Margaret TM and Simons J: Nuclear expression of hypoxia-inducible factor 1alpha protein is heterogeneous in human malignantcells under normoxic conditions. Cancer Lett 181: 233, 2002.
6. Wang Y, Wan C, Deng L, *et al*: The hypoxia-inducible factor alpha pathway couples angiogenesis to osteogenesis during skeletal development. J Clin Invest 117: 1616-1626, 2007.
7. Giaccia A, Siim BG and Johnson RS: HIF-1 as a target for drug development. Nat Rev Drug Discov 2: 803-811, 2003.
8. Diab T, Pritchard EM, Uhrig BA, Boerckel JD, Kaplan DL and Guldberg RE: A silk hydrogel-based delivery system of bone morphogenetic protein for the treatment of large bone defects. J Mech Behav Biomed Mater 11: 123-131, 2012.
9. Wigner NA, Luderer HF, Cox MK, Sooy K, Gerstenfeld LC and Demay MB: Acute phosphate restriction leads to impaired fracture healing and resistance to BMP-2. J Bone Miner Res 25: 724-733, 2010.
10. Kim TH, Oh SH, Na SY, Chun SY and Lee JH: Effect of biological/physical stimulation on guided bone regeneration through asymmetrically porous membrane. J Biomed Mater Res A 100: 1512-1520, 2012.
11. Chang SC, Lin TM, Chung HY, *et al*: Large-scale bicortical skull bone regeneration using ex vivo replication-defective adenoviral-mediated bone morphogenetic protein-2 gene-transferred bone marrow stromal cells and composite biomaterials. Neurosurgery 65: 75-81, 2009.
12. Liu Y, Lu Y, Tian X, *et al*: Fragmental bone regeneration using an rhBMP-2-loaded gelatin/nanohydroxyapatite/fibrin scaffold in a rabbit model. Biomaterials 30: 6276-6285, 2009.
13. Baltzer AW, Ostapczuk MS, Stosch D and Granrath M: The use of recombinant human bone morphogenetic protein-2 for the treatment of a delayed union following femoral neck open-wedge osteotomy. Orthop Rev (Pavia) 4: e4, 2012.
14. Kanczler JM, Ginty PJ, White L, *et al*: The effect of the delivery of vascular endothelial growth factor and bone morphogenic protein-2 to osteoprogenitor cell populations on bone formation. Biomaterials 31: 1242-1250, 2010.
15. Kang SW, Bae JH, Park SA, *et al*: Combination therapy with BMP-2 and BMSCs enhances bone healing efficacy of PCL scaffold fabricated using the 3D plotting system in a large fragmental defect model. Biotechnol Lett 34: 1375-1384, 2012.
16. Simon F, Bockhorn M, Praha C, *et al*: Deregulation of HIF1-alpha and hypoxia- regulated pathways in hepatocellular carcinoma and corresponding non-malignant liver tissue--influence of a modulated host stroma on the prognosis of HCC. Langenbecks Arch Surg 395: 395-405, 2010.
17. Lando D, Peet DJ, Whelan DA, Gorman JJ and Whitelaw ML: Asparagine hydroxylation of the HIF transactivation domain a hypoxic switch. Science 295: 858-861, 2002.
18. Lim W, Cho J, Kwon HY, Park Y, Rhyu MR and Lee Y: Hypoxia-inducible factor 1 alpha activates and is inhibited by unoccupied estrogen receptor beta. FEBS Lett 583: 1314-1318, 2009.
19. Elson DA, Thurston G, Huang LE, *et al*: Induction of hypervascularity without leakage or inflammation in transgenic mice overexpressing hypoxia-inducible factor-1alpha. Genes Dev 15: 2520-2532, 2001.
20. Liu DP, Wang GX, Hu L and Li C: Construction of adenovirus-mediated eukaryotic expression vector co-expressing mutant hypoxia-inducible factor-1 alpha target protein and humanized Renilla reniformis green fluorescent protein reporter molecule under normoxic conditions. J Clin Rehab Tiss Eng Res 14: 3787-3792, 2010.